Chapter

Maximum Power Point Tracking for Thermoelectric Generators Using Their Accurate Electrothermal Model

Mohammad Javad Dousti[1*], Antonio Petraglia[2] and Massoud Pedram[1]

[1]University of Southern California, Los Angeles, CA, US

[2]Federal University of Rio de Janeiro, Rio de Janeiro, RJ, Brazil

Abstract

Thermoelectric generators (TEGs) provide a unique way for harvesting thermal energy. These devices are compact, durable, inexpensive, and scalable. Unfortunately, the energy conversion efficiency of TEGs is low. This requires careful design of energy harvesting systems including the interface circuitry between the TEG module and the load, with the purpose of minimizing power losses. In this chapter, it is analytically shown that the traditional approach for estimating the internal resistance of TEGs may result in a significant loss of harvested power. This drawback comes from ignoring the dependence of the electrical behavior of TEGs on their thermal behavior. Accordingly, a systematic method for accurately determining the TEG input resistance is presented. Based on this method, a maximum power point tracking algorithm for TEGs is presented which only utilizes temperature sensors' data in order to adjust the interface circuitry. A tracking method is necessary to offset the effect of temperature change across TEG junctions on TEGs' input resistance.

PACS: 05.45-a, 52.35.Mw, 96.50.Fm

Keywords: Thermoelectric Generator, Modeling, Electrothermal

1. Introduction

Energy harvesting has gained significant attention due to the ever increasing demand for energy. Harvested energies are usually renewable energies (such as solar, wind, etc.) or

[*]E-mail address: dousti@usc.edu.

otherwise wasted energies (like heat) [1]. Abundance and availability at no cost make harvesting of the electrical energy out of those sources quite attractive. One of such energy sources is heat, which can be converted into electricity by means of *thermoelectric generators* (TEGs). TEGs work based on the *Seebeck effect*, which converts a temperature gradient into a voltage.

TEGs have unique capabilities, which have made them a preferable choice compared to conventional energy sources (such as batteries) and other energy harvesting methods (such as solar cells). TEGs are:

1. *Silent:* TEGs have no moving part and are made of semiconductor materials and hence, generate no noise [2].
2. *Very durable:* TEGs are reported to work for up to 30 years [2], which makes them ideal for remote or difficult-to-reach locations and the outer space. For space missions beyond Mars, TEGs are the only means of energy harvesting, since the sunlight intensity drops significantly [3].
3. *Compact and lightweight:* Each TEG can be manufactured to be as small as $0.5mm \times 0.5mm \times 100\mu m$ [4].
4. *Inexpensive:* The cost of deploying TEGs compared to large generators or batteries (considering the replacement cost) is quite low [5].
5. *Scalable:* TEG modules can be simply connected together to increase the amount of harvested energy [2].

Despite the aforesaid appealing characteristics, TEGs suffer from low conversion efficiency, which is imposed by two main factors. First, the *Carnot cycle efficiency*, which sets a theoretical upper bound on the conversion efficiency of thermal energy to work, can be quite low. Specifically, this efficiency is defined as $\eta_{Carnot} = \Delta T/T_h$, where T_h is the temperature of the hot side and ΔT is the temperature difference between hot and cold sides. Clearly, when ΔT is small, the conversion efficiency is quite low. For instance, 30K temperature difference in the room temperature (300K) can provide up to 10% efficiency. The second limiting factor is the efficiency of the thermoelectric effect. The overall TEG efficiency can be formulated as [2]

$$\eta_{TEG} = \frac{\Delta T}{T_h} \cdot \frac{\sqrt{1+ZT_{avg}}-1}{\sqrt{1+ZT_{avg}}+T_c/T_h}, \tag{1}$$

where Z is the TEG *figure of merit* and $T_{avg} = (T_h + T_c)/2$. State-of-the-art TEGs have ZT_{avg} value of 2.1 for $T_{avg} = 300K$ (27°C) [4]. For the same temperature difference used above, the efficiency of this TEG is equal to only 2.8%, which is 72% lower than that of an ideal Carnot cycle. Evidently, the efficiency of TEGs is quite low. Low efficiency limits the usage of TEGs to low-power applications. Note that usually the overall energy of the source is rather low. For instance, you may consider the heat generated from the human body. This factor also limits the amount of harvested energy. Devices with power consumption of 100mW or less are ideal targets to be powered by thermoelectric generators, whereas devices with higher power consumption require larger temperature gradient in order to be powered by TEGs.

The process of converting the temperature difference to usable electrical energy involves two steps. First, TEGs convert the temperature difference into an electrical voltage which is usually not suitable for the load and needs to be regulated. Next, this voltage is converted by an interface circuit to a regulated voltage required by the load or the energy storage element. This process is shown in Figure 1. Note that in order to extract the maximum power from the generator and transfer it to the load, the interface circuit input resistance (R^{in}_{iface}) must be matched to the TEG internal resistance ($R^{in}_{TEG,N}$). This step is necessary to avoid losses in an already-low harvested energy.

In the prior art (such as [1, 3, 6, 7]), $R^{in}_{TEG,N}$ was set to be equal to the electrical resistance of the thermoelectric module ($R_{TEG,N}$). In this chapter, we first develop an electro-thermal model of TEGs. Using this model, an analytical methodology for determining $R^{in}_{TEG,N}$ is presented. Next, a *maximum power point tracking* (MPPT) algorithm for TEGs is presented which only utilizes temperature sensors' data in order to adjust the interface circuitry. A tracking method is necessary to offset the effect of temperature change across TEG junctions on its input resistance. Accordingly, the suggested tracking algorithm works based on the proposed method for determining the TEG input resistance.

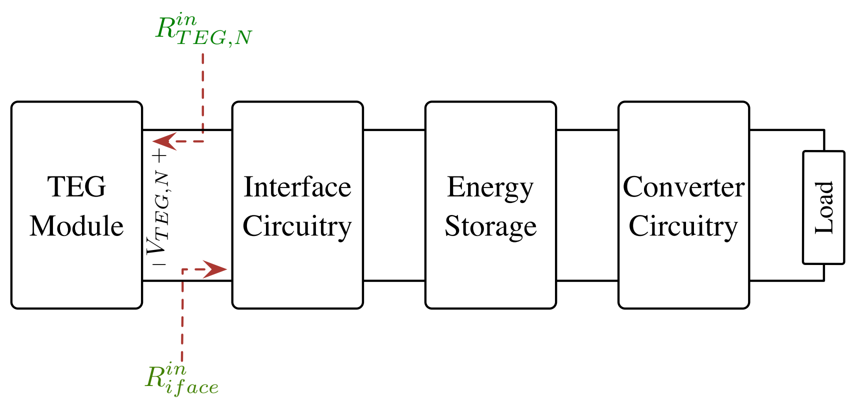

Figure 1. High-level structure of a TEG harvesting system.

This manuscript extends our previous work [8] by proposing a new MPPT algorithm for TEGs based on the suggested accurate electro-thermal model for them. Accordingly, the MPPT method only requires temperature sensors as opposed to other methods which are based on voltage or current sensors. Consequently, it does not frequently disconnect the TEG module from the rest of the system in order to measure its open circuit voltage.

The remainder of this paper is organized as follows. Section 2 describes prior work. Next, Section 3 presents an electro-thermal model for TEGs and derive a methodology for determining their input resistances. After that, Section 4 analyzes the sensitivity of the TEG internal resistance on device parameters and the temperature across its junctions. Then, Section 5 presents an MPPT algorithm suitable for TEGs. Finally, Section 6 concludes the paper.

2. Previous Work

Research on thermoelectric generators is mainly divided into two parts. First, the manufacturing and assembly techniques in order to maximize TEG's figure of merit. Second, designing the interface circuit for maximally transferring the generated power to the load. The focus of this paper is on the latter part.

Much work has been conducted on designing interface circuits. Even though the electro-thermal model of TEGs are constructed (e.g., [9]), the internal resistance of N TEGs ($R^{in}_{TEG,N}$) is claimed to be equal to the electrical resistance of the thermoelectric material and its associated contacts ($R_{TEG,N}$). This modeling neglects the thermal resistance of TEG contacts and its effects on $R^{in}_{TEG,N}$. Here we enumerate a few examples that consider $R^{in}_{TEG,N}$ to be equal to $R^{in}_{TEG,N}$.

Books [1] and [3] explain the basic equations for the amount of power that can be extracted from TEGs. In order to maximize the extracted power, they claim that the load should be matched with electrical resistivity of a TEG module. Solbrekken *et al.* [6] also use the electrical resistance of TEGs and adopt it as a relation to determine the internal resistance of TEGs. Lu *et al.* [7] use the electrical resistivity of TEGs to make a Thevenin equivalent circuit. As we will explain later, since TEGs are non-linear circuits, the Thevenin theorem does not apply to them.

There are many MPPT techniques developed mostly for photovoltaics, such as *current sweep*, *fractional V_{OC} and I_{SC}*, *array reconfiguration*, etc. Some of these techniques are general and can be used for TEGs as well. However, most of the techniques require sensing of open circuit voltage ($V^{oc}_{TEG,N}$), current (I), or both. Esram *et al.* [10] provide an excellent survey of these methods. On the other hand, the MPPT algorithm proposed in this paper only requires temperature sensors. Consequently, this algorithm does not require to periodically disrupt and disconnect the power harvesting module in order to sense the open circuit voltage.

3. Analytical Modeling of TEG Input Resistance

In this section, first an electro-thermal model of a TEG module is described. Next, considering the contact thermal and electrical resistances, we use this model to derive an accurate methodology for determining $R^{in}_{TEG,N}$.

3.1. TEG Electro-Thermal Model

Thermoelectric generators are compact devices, which are made of pairs of N- and P-type semiconductor pellets. Usually, these pellets are fabricated from properly doped Bismuth Telluride (Bi_2Te_3). When a temperature difference is applied across these pellets, current flows through pellets due to the *Seebeck effect*. The direction of generated current in an N-type pellet is opposite of that of a P-type pellet. Hence, to improve the amount of harvested energy and increase the overall generated voltage ($V_{TEG,N}$), these pellets are connected in a zig-zag manner, i.e., they are connected electrically in series and thermally in parallel. Figure 2 depicts a 3×3 array of TEG pellet pairs (a total of 9 pairs) connected to a load, which is usually a converter circuitry to interface between TEG and the energy storage.

When a temperature gradient is applied to this module such that the bottom side (*hot side*) becomes hotter than the top side (*cold side*), current flows through the load in the clockwise direction.

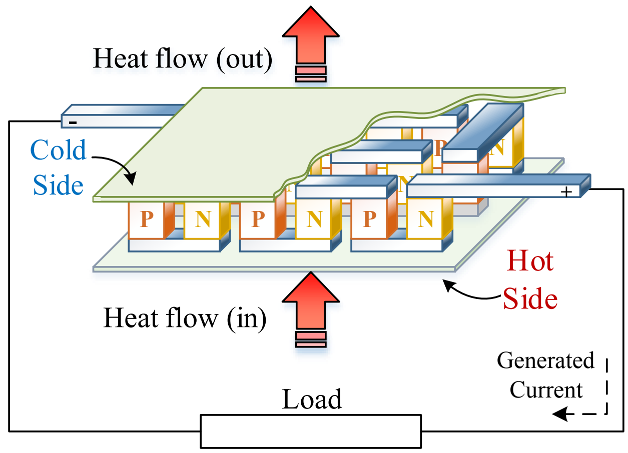

Figure 2. A 3 × 3 TEG module connected to a load.

The total electrical resistance of a TEG pellet can be calculated as

$$R_{TEG} = 4R_{cont} + R_{SL}, \tag{2}$$

where R_{cont} is the contact resistance plus the resistance between a semiconductor pellet and its respective metal contact and R_{SL} is the electrical resistance of N- and P-pellets. The multiplier factor of 4 on the first term accounts for four contact surfaces between pellets and contacts.

The generated voltage by TEGs is called *Seebeck voltage* and can be formulated as

$$\alpha_N \Delta T, \tag{3}$$

where α_N is the *Seebeck coefficient* of N pellet pairs and ΔT is the temperature difference across them. The heat flow rate through the hot side of a TEG module ($\dot{q}_h$) and its cold side ($\dot{q}_c$) which result in the generation of current I may be formulated as

$$\dot{q}_h = \frac{\Delta T}{\Theta_{TEG,N}} - \alpha_N I T_h - \frac{1}{2} R_{TEG,N} I^2 \quad \text{and} \tag{4}$$

$$\dot{q}_c = \frac{\Delta T}{\Theta_{TEG,N}} - \alpha_N I T_c + \frac{1}{2} R_{TEG,N} I^2. \tag{5}$$

In these equations, $R_{TEG,N}$ and $\Theta_{TEG,N}$ are the electrical and thermal resistances of N pairs of TE pellets. In this paper, the subscript N denotes a parameter describing N TE pairs, whereas parameters without it are related to only one pair. Accordingly, we have $\alpha_N = N \times \alpha$, $R_{TEG,N} = N \times R_{TEG}$, and $\Theta_{TEG,N} = \Theta_{TEG}/N$.

Using the well-known duality between electrical and thermal phenomena [11], an electro-thermal model of N TEGs can be developed as shown in Figure 3 [9]. Note that the red part shows the thermal model, whereas the blue part designate the electrical model.

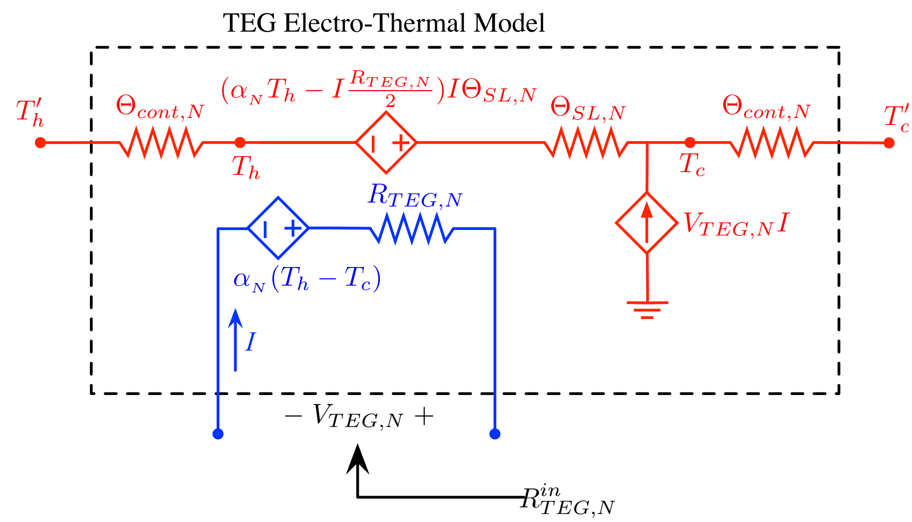

Figure 3. Electro-thermal model of N TEGs considering the contact thermal resistances. The thermal part is represented in red and the electrical part is shown in blue.

In Figure 3, $\Theta_{SL,N}$ represents the thermal resistivity of N super-lattice material pairs, whereas $\Theta_{cont,N}$ shows the thermal resistivity of metal contacts on the top or bottom of N TEGs. Clearly, the following relation holds.

$$\Theta_{TEG,N} = \Theta_{cont,N} + \Theta_{SL,N} = N(\Theta_{cont} + \Theta_{SL}) \tag{6}$$

Note that each pellet is connected to two metal contacts which can be modeled by two series resistors with the value of Θ_{cont}; however, pairs of pellets are thermally connected in parallel. Hence, the overall contact thermal resistance for a pair of pellets is equal to Θ_{cont}.

3.2. Maximum Power Transfer

As can be seen in Figure 3, a TEG is subjected to a temperature differential through its metal contacts. The thermal and electrical contact resistances of TEGs are not negligible [4]. The contact thermal resistance ($\Theta_{cont,N}$) causes the temperature at surfaces of a TEG module (i.e., T_c' and T_h') differ from the temperature on the N- and P-type pellets (i.e., T_c and T_h). Assuming that T_c' and T_h' are set externally, values of T_c and T_h become dependent on the parameters of TEG shown in the thermal part. Consequently, this affects the internal resistance of the TEG. In order to determine the internal resistance, the usual procedure consists in deriving a Thevenin equivalent circuit. However, the electro-thermal model of TEGs is a non-linear circuit. The non-linearity is produced in the thermal part, where a current-controlled voltage source generates a voltage that is a quadratic function of the current I in the electrical circuit. Hence, the Thevenin's theorem cannot be applied to this circuit.

Therefore, we directly find the load resistance seen by the TEG module that maximizes the power consumed in the load. Note that the maximization of *conversion efficiency* of TEGs is a different objective. Efficiency is maximized for large values of the load resistance

[12]. However, since the TEG source energy (i.e., heat) is available for free, the conversion efficiency is not of interest and hence the objective is to maximize the power transferred to the load.

Suppose the interface circuit has the input resistance R^{in}_{iface} seen from the outputs of the TEG module. $V_{TEG,N}$ and I denote the voltage and the current, respectively, at R^{in}_{iface}. Clearly, the following optimization problem should be solved to find the optimal R^{in}_{iface} (called R^{in*}_{iface}).

$$R^{in*}_{iface} = \underset{R^{in}_{iface}}{\mathrm{argmax}}\{V^2_{TEG,N}/R^{in}_{iface}\} \tag{7}$$

According to the *maximum power transfer theorem* [12], the internal resistance of TEG module ($R^{in}_{TEG,N}$) should be equal to R^{in*}_{iface}.

Using the nodal analysis, $V_{TEG,N}$ as a function of I can be calculated as shown below.

$$\begin{aligned} V_{TEG,N} = &\left(\frac{\alpha_N R^{in}_{iface}\Theta_{SL,N}}{R^{in}_{iface} + R_{TEG,N}}\right) \times \\ &\left(\frac{T'_h - T'_c + \alpha_N I \Theta_{cont,N}(I^2\Theta_{cont,N}R_{\mathrm{TEG,N}} + T'_h + T'_c)}{2\Theta_{cont,N} + \Theta_{SL,N} - \alpha^2_N I^2 \Theta^2_{cont,N}\Theta_{SL,N}}\right) \end{aligned} \tag{8}$$

As expected,

$$\lim_{\Theta_{cont}\to 0} V_{TEG,N} = \alpha_N(T'_h - T'_c)\frac{R^{in}_{iface}}{R^{in}_{iface} + R_{TEG,N}}, \tag{9}$$

indicating that as the thermal contact resistance tends to zero, T'_h and T'_c approach T_h and T_c, respectively.

Note that we also have

$$V_{TEG,N} = -IR^{in}_{iface}. \tag{10}$$

Solving the system of equations comprised of (8) and (10) yields an equation for $V_{TEG,N}$ independent of I. By substituting the derived $V_{TEG,N}$ into Eq. (7) and solving the resulting equation, we obtain three solutions of which only one is real valued. This real solution has a closed-form expression in terms of TEG parameters; however, it is lengthy and we omit it for brevity. Using the derived value for R^{in*}_{iface} (or equivalently $R^{in}_{TEG,N}$), *maximum power extraction* (MPE) can be performed for TEGs.

4. Sensitivity Analysis

This section analyzes the sensitivity of the TEG internal resistance on TEG parameters and the temperature applied to its junctions. We consider a thermoelectric module made by *Kryotherm* called *TB-127-1.4-1.2* [13]. Physical parameters of this module are as follows: $N = 127$, $\alpha = 418.8\mu V/K$, $R_{TEG} = 12.6m\Omega$, $\Theta_{SL} = 190.3K/W$, and $\Theta_{cont} = 57.2K/W$.

Synopsys HSPICE was used for performing circuit simulations. After developing the method for determining $R^{in}_{TEG,N}$, we verified the theoretical analysis by comparing the result with SPICE simulations. Perfect agreement was observed.

The baseline value for the sensitivity analysis is $R_{TEG,N} = 1.6\Omega$ ($R_{TEG} \times N$). Accordingly, we measure how much $R_{TEG,N}$ differs from the actual internal resistance ($R^{in}_{TEG,N}$) by reporting $\Delta R/R^{in}_{TEG,N}$, where $\Delta R = R^{in}_{TEG,N} - R_{TEG,N}$. We refer to this metric as *resistance mismatch ratio*.

In all analyses, the TEG parameters presented earlier are fixed and T'_c and T'_h are set to 27°C and 57°C, respectively. Then, one or two parameters are selected at a time and varied. Note that the figure of merit introduced in Section 1 is defined as $Z = \alpha^2\Theta_{TEG,N}/R_{TEG,N}$. This means that increasing α and $\Theta_{TEG,N}$ and reducing $R_{TEG,N}$ improve the figure of merit of a TEG. Accordingly, we change these parameters and study their effect on $R^{in}_{TEG,N}$.

First, we select N and R_{TEG} parameters for analysis. However, it turns out that these parameters affect both $R^{in}_{TEG,N}$ and $R_{TEG,N}$ in the same way. In other words, $\Delta R/R^{in}_{TEG,N}$ remains constant. Next, we change the value of α. The result of this analysis is shown in Figure 4. As can be seen, the resistance mismatch ratio increases almost linearly with incrementing α.

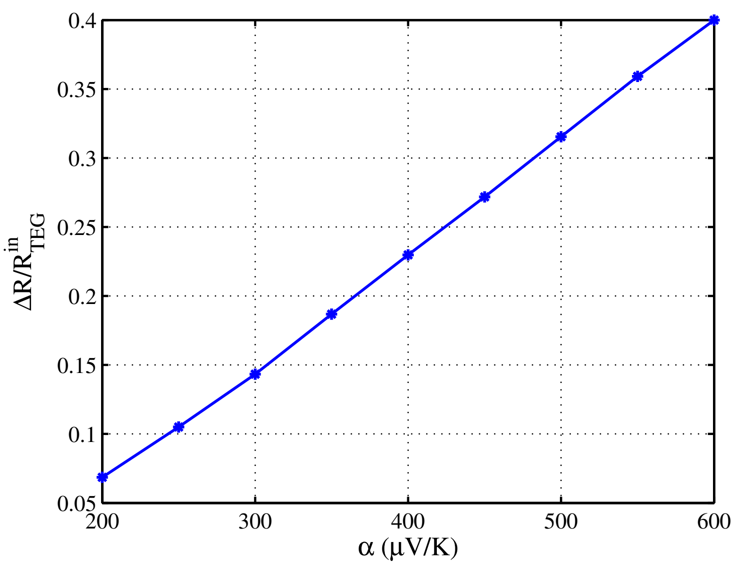

Figure 4. Sensitivity analysis of resistance mismatch ratio on the Seebeck coefficient.

Next, we consider Θ_{SL} and Θ_{cont}. As observed in Figure 3, these two parameters realize a voltage divider between T'_c and T'_h. Hence, we analyze them together. Accordingly, we choose three values for Θ_{cont} and vary Θ_{SL} to investigate how changing the ratio of $\Theta_{SL}/\Theta_{cont}$ affects the resistance mismatch ratio. Figure 5 depicts the result. As illustrated, growth of both parameters increases the resistance mismatch ratio; however, parameter Θ_{cont} has more noticeable effect. This complies with our expectation; increasing Θ_{cont} results in larger difference between temperatures on TEG contacts (T'_c and T'_h) and TEG super-lattices (T_c and T_h).

Note that usually the value of α, Θ_{SL}, and R_{TEG} are physically correlated [1]. That's why fabricating TEGs with large figure of merit is difficult. In this paper, our aim was to forecast the effect of using TEGs with larger figure of merit values on the resistance

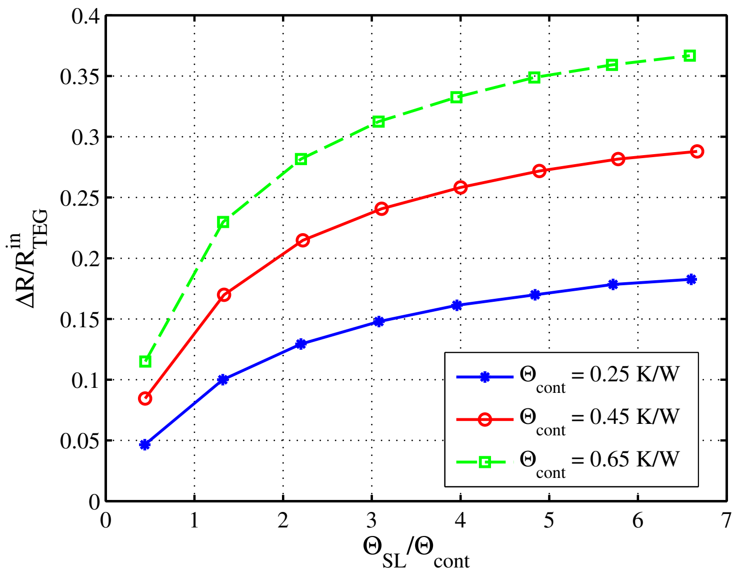

Figure 5. Sensitivity analysis of resistance mismatch ratio on the TEG contact and supper-lattice thermal resistivity.

mismatch ratio.

Finally, we consider the effect of varying temperature. Figure 6 shows the result of changing T'_c and $\Delta T' = T'_h - T'_c$ on the resistance mismatch ratio. As can be seen, changing T'_c has more significant effect on the resistance mismatch ratio compared to $\Delta T'$. On the other hand, $\Delta T'$ is the key parameter (along with α), which determines $V_{TEG,N}$. With radical change in temperature, $R_{TEG,N}$ would be more than 50% smaller than the actual internal resistance ($R^{in}_{TEG,N}$).

5. Maximum Power Point Tracking

The temperature of the cold and hot sides of a TEG module can be changed during its operation which affect the TEG internal resistance. As a result, during the design stage, the range of temperature change should be determined. Accordingly a *maximum power point tracking* (MPPT) system might be required to dynamically adjust the input resistance of the interface circuit in case the temperature variation range is significant. Note that when the temperature difference changes, $V_{TEG,N}$ and I also vary (see Equations (3) and (10)).

Using the exemplary device from the previous section, Figure 7 depicts the amount of harvested power as a function of current drawn for various values of $\Delta T'$ and T'_c. Blue dots show points where the harvested power is maximized. These high temperature values (and even larger values) are common in *automotive thermoelectric generators* (ATEGs), where the heat generated by the internal combustion engine is converted into electricity [1, 3, 14, 15].

As can be seen in Figure 7, the optimum current values (i.e., the current associated with the maximum harvested power) vary significantly when temperature changes. Hence,

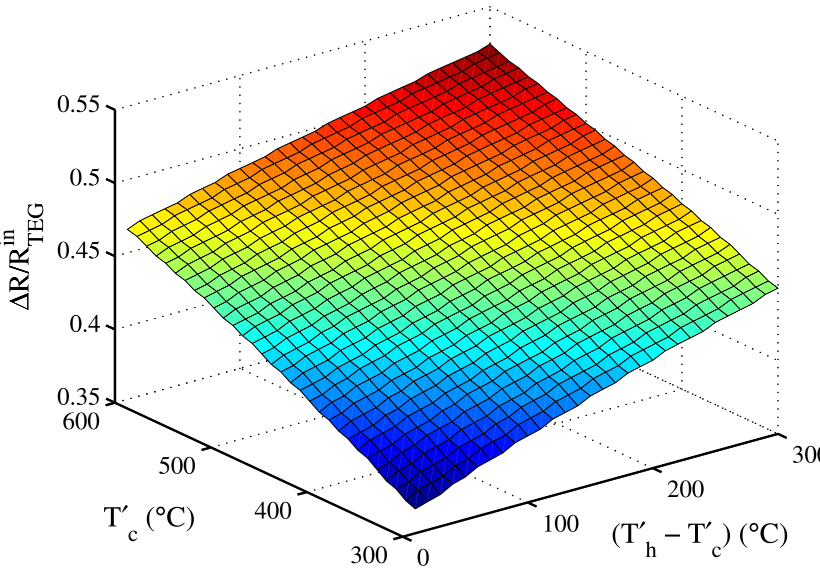

Figure 6. Sensitivity analysis of resistance mismatch ratio on the hot and cold site temperatures of a TEG module.

an MPPT technique is required for ATEGs to offset the variation of temperature. With the model provided in Section 3(B), one can derive R^{in*}_{iface} and accordingly calculate the optimum current and voltage. Next, these value can be used to adjust the interface circuitry to match the TEG module input resistance (see Figure 1). This interface circuitry is usually an adjustable buck, boost, or buck-boost converter [10].

Based on the above discussion, Algorithm 1 presents an MPPT technique specifically designed for TEGs. This algorithm only requires the value of temperature sensors and does not necessitate to periodically disrupt and disconnect the power harvesting module in order to sense $V^{oc}_{TEG,N}$.

Algorithm 1 Maximum Power Point Tracking for TEGs

Input: α_N, $\Theta_{SL,N}$, $R_{TEG,N}$, and temperature sensor values
Output: MPPT control signal

1: **while** *TRUE* **do**
2: Measure T'_c and T'_h
3: Find $R^{in}_{TEG,N}$ from the method presented in Section 3(B)
4: Determine the appropriate PWM signal to control the MPPT circuitry in order to have an internal resistance equal to $R^{in}_{TEG,N}$
5: **end while**

The proposed algorithm comprises of a control loop (lines 1 and 5) where it periodically senses T'_c and T'_h (line 2). Note that T_c and T_h values cannot be sensed directly. Accordingly, it finds the internal resistance of the TEG module (line 3). Knowing the value of

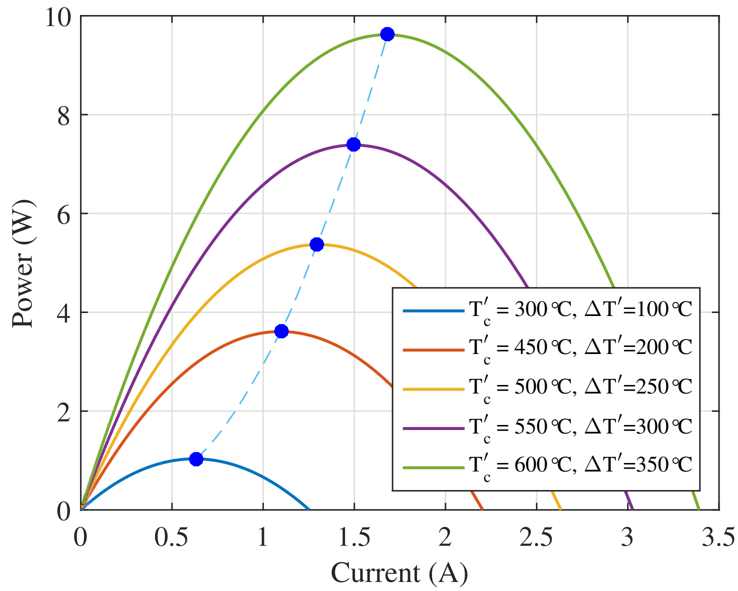

Figure 7. Harvested power as a function of current drawn for various values of ΔT and T_c.

the internal resistance, a controlling PWM signal can be generated to adjust R^{in}_{iface} of the interface circuitry to be equal to $R^{in}_{TEG,N}$ (line 4). Details of the last step is outside the scope of this paper and can be found in the literature.

6. Conclusion

In this paper, it was analytically shown that the effective internal resistance of TEGs can vary from its electrical resistance by more than 50%. This difference comes from ignoring the dependence of the electrical behavior of TEG on its thermal behavior. Accordingly, a systematic method for accurately determining the TEG input resistance was developed. Based on this method, a maximum power point tracking algorithm was presented to offset the effect of temperature variation on the input resistance.

Acknowledgment

This project is funded in part by the Computer Systems program of the Division of Computer and Network Systems of the US NSF CISE, and the Brazilian research agencies CAPES, CNPq, and FAPERJ.

References

[1] S. Beeby and N. White, Eds., Energy Harvesting for Autonomous Systems. Artech House, 2010.

[2] G. J. Snyder, Small thermoelectric generators, Electrochemical Society Interface, pp. 5557, 2008.

[3] D. M. Rowe, Ed., Thermoelectrics Handbook: Macro to Nano, 1st ed. CRC Press, Dec. 2005.

[4] I. Chowdhury, R. Prasher, K. Lofgreen, G. Chrysler, S. Narasimhan, R. Mahajan, D. Koester, R. Alley, and R. Venkatasubramanian, On-chip cooling by superlatticebased thin-film thermoelectrics, Nature Nanotechnology, vol. 4, no. 4, pp. 235 238, 2009.

[5] Y. Ramadass and A. Chandrakasan, A battery-less thermoelectric energy harvesting interface circuit with 35 mv startup voltage, IEEE Journal of Solid-State Circuits, vol. 46, no. 1, pp. 333 341, Jan 2011.

[6] J. A. Federici, D. G. Norton, T. Brüggemann, K. Voit, E. Wetzel, and D. Vlachos, Catalytic microcombustors with integrated thermoelectric elements for portable power production, Journal of Power Sources, vol. 161, no. 2, pp. 1469 1478, 2006.

[7] C. Lu, S. P. Park, V. Raghunathan, and K. Roy, Analysis and design of ultra low power thermoelectric energy harvesting systems, in Proc. of the International Symposium on Low-Power Electronics and Design, Aug 2010, pp. 183 188.

[8] M. J. Dousti, A. Petraglia, and M. Pedram, Accurate electrothermal modeling of thermoelectric generators, in Proc. of the Design, Automation & Test in Europe Conference, 2015, pp. 1603 1606.

[9] S. Lineykin and S. Ben-Yaakov, Analysis of thermoelectric coolers by a spicecompatible equivalent-circuit model, IEEE Power Electronics Letters, vol. 3, no. 2, pp. 63 66, 2005.

[10] T. Esram, P. L. Chapman et al., Comparison of photovoltaic array maximum power point tracking techniques, IEEE Transactions on Energy Conversion, vol. 22, no. 2, p. 439, 2007.

[11] M. Pedram and S. Nazarian, Thermal modeling, analysis, and management in vlsi circuits: Principles and methods, Proceedings of the IEEE, vol. 94, no. 8, pp. 1487 1501, 2006.

[12] D. W. Hart, Power electronics. McGraw -Hill Education, 2011.

[13] Kryotherm. [Online]. Available: http://www.kryotherm.com.

[14] L. E. Bell, Cooling, heating, generating power, and recovering waste heat with thermoelectric systems, Science, vol. 321, no. 5895, pp. 1457 1461, 2008.

[15] TEGs - using car exhaust to lower emissions. [Online]. Available: http://www.science20.com/news releases/tegs using car exhaust to lower emissions.